Interaction-free measurement as quantum channel discrimination

You Zhou[1] and Man-Hong Yung[2,3,1,*]

[1]*Center for Quantum Information, Institute for Interdisciplinary Information Sciences, Tsinghua University, Beijing 100084, China*

[2]*Institute for Quantum Science and Engineering and Department of Physics, South University of Science and Technology of China, Shenzhen 518055, China*

[3]*Shenzhen Key Laboratory of Quantum Science and Engineering, Shenzhen 518055, China*

(Received 24 August 2017; published 22 December 2017)

Interaction-free measurement is a quantum process where, in the ideal situation, an object can be detected as if no interaction took place with the probing photon. Here we show that the problem of interaction-free measurement can be regarded as a problem of quantum-channel discrimination. In particular, we look for the optimal photonic states that can minimize the detection error and the photon loss in detecting the presence or absence of the object, which is taken to be semitransparent, and the number of the interrogation cycle is assumed to be finite. Furthermore, we also investigated the possibility of minimizing the detection error through the use of entangled photons, which is essentially a setting of quantum illumination. However, our results indicate that entanglement does not exhibit a clear advantage; the same performance can be achieved with unentangled photonic states.

DOI: 10.1103/PhysRevA.96.062129

I. INTRODUCTION

Quantum measurement is a fundamental concept in quantum theory. The measurement process extracts the information stored in a quantum system to the classical world. In many scenarios, measurement on the target system, say A, is accomplished indirectly by coupling it to another system B. However, even the nonobservance of a particular result of B would modify the quantum state of A, which is called the "negative result measurement" [1,2]. In addition, Elitzur and Vaidman introduced a "counterfactual" protocol, called interaction-free measurement (IFM) [3]. In this protocol, a photon is sent to a standard Mach-Zehnder interferometer to detect an opaque object, where the maximum efficiency for a successful detection without photon absorption is 50% [3,4]. However, by a modification on account of the quantum Zeno effect [5], the efficiency can approach 100% as the interrogation cycle goes to infinity [4,6]. Interaction-free measurement has been applied to detecting fragile objects, such as individual atom [7,8] or photon-sensitive substances [9], and even electron microscopy [10–12].

Apart from the original optical setup [4,6], there are several theoretical proposals [10,13–15] and experimental demonstrations [16–18] for achieving "quantum-Zeno-like" IFM. The physical model behind them is essentially the same; they all utilized the quantum Zeno effect to keep the photon state unchanged, in the presence of an object.

Here we consider a more general scenario, where we consider the problem of detecting the object as a problem of channel discrimination, which means that we aim at minimizing the error rate in identifying the presence of a target. We shall consider all possible input states, including entangled states, for the incident photon, and at the end the best positive operator-valued measure (POVM) measurement for minimizing the detection error.

To be specific, we focus on the same optical setup as in Ref. [6] to illustrate our main results (see Fig. 1). In particular, our paper takes into account the possibility that the photon may be lost in the middle of the detection process. Let us denote, respectively, the states $|1\rangle$, $|2\rangle$, and $|3\rangle$ as the representation for

$$\text{up} \Leftrightarrow |1\rangle, \quad \text{down} \Leftrightarrow |2\rangle, \quad \text{loss} \Leftrightarrow |3\rangle \tag{1}$$

states of the incident photon. A light-absorbing object (e.g., a photon-sensitive explosive in Ref. [3]) is placed in the path of the down state photon. And the probability for this object to appear is denoted by $\Pr(\text{here}) = q$.

In fact, in order to describe the photon state transformation when the object is present explicitly, we shall mimic the effect of the object with a mirror, followed by a photon detector [4] (see Fig. 1 for detailed illustration).

A. Interaction-free measurement

Let us first summarize the essential idea of the standard interaction-free measurement: first, an incident photon is prepared in the up path, with a quantum state labeled by $|1\rangle$. Then, the incident photon is rotated by an angle θ through a beamsplitter,

$$R_\theta|1\rangle = \cos\theta|1\rangle + \sin\theta|2\rangle, \tag{2}$$

where

$$\theta \equiv \frac{\pi}{2N} \tag{3}$$

depends on N, the total number of interrogation cycles.

1. Presence of the object

If there exists an object along the down path, the photon in the down state $|2\rangle$ will be completely transferred to the lost state $|3\rangle$ by the mirror, i.e.,

$$U_{\rm I}|2\rangle = |3\rangle, \tag{4}$$

where the subscript of $U_{\rm I}$ stands for interaction. Furthermore, when applying it to a quantum superposition, we have

$$U_{\rm I}(\cos\theta|1\rangle + \sin\theta|2\rangle) = \cos\theta|1\rangle + \sin\theta|3\rangle. \tag{5}$$

*yung@sustc.edu.cn

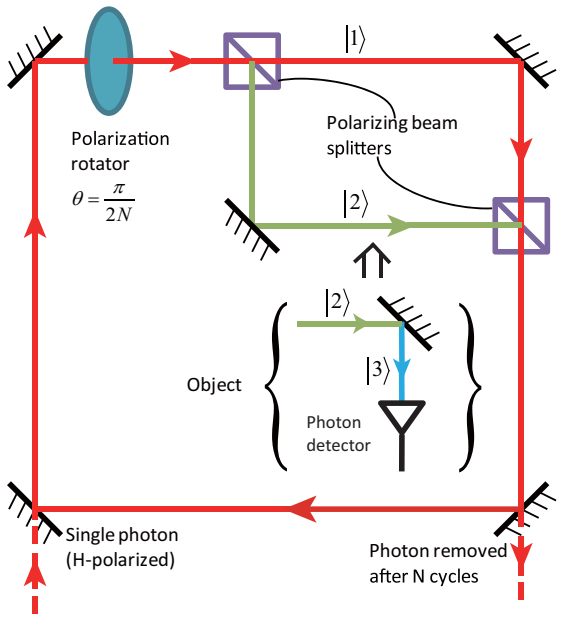

FIG. 1. The "quantum-Zeno-like" IFM setup. We illustrate the principle of IFM using the optical scheme in Ref. [6]. The polarization rotator rotates the photon polarization by $\theta = \frac{\pi}{2N}$ in each cycle. And the polarizing beamsplitter separates the photon to an up or down path if the photon is horizontal polarized H or vertical polarized V. So the polarizations of the photon label the up state $|1\rangle$ and the down state $|2\rangle$ in Eq. (1), respectively. In addition, the object is mimicked with a mirror followed by a photon detector. The mirror transforms the down state $|2\rangle$ to the loss state $|3\rangle$. And the photon detector implements the projective measurement on the two $\{|1\rangle,|2\rangle\}$ and $\{|3\rangle\}$ subspaces. As interrogation cycle N goes to infinity, we can judge whether there is an object in the down path with the final polarization state of the photon, without any photon absorption.

Then, followed by the projective measurement of the photon detector,

$$P_0 = |1\rangle\langle 1| + |2\rangle\langle 2|,$$
$$P_1 = |3\rangle\langle 3|, \tag{6}$$

the final state in Eq. (5) becomes a mixed state,

$$\cos^2\theta|1\rangle\langle 1| + \sin^2\theta|3\rangle\langle 3|, \tag{7}$$

where the probability of the photon traveling along the up path without absorption is given by $\Pr(|1\rangle) = \cos^2\theta$. And the probability that the photon is transformed to the loss state $|3\rangle$ and absorbed by the detector is $\Pr(|3\rangle) = \sin^2\theta$.

In the probability subspace of P_1, the lost photon does not participate in the following interrogation cycle, i.e., the IFM process halts in this case. Consequently, the probability of finding $|1\rangle$ after N cycles equals to $\Pr(|1\rangle) = \cos^{2N}(\theta)$. When N approaches infinity, we have

$$\lim_{N\to\infty} \cos^{2N}(\theta) = 1. \tag{8}$$

Therefore, one can find the final state to be $|1\rangle$ with probability 1 without any photon loss, in the presence of an object.

2. Absence of the object

If there is no object, i.e., the down state $|2\rangle$ will travel straight through without getting absorbed (or reflected by the mirror), the rotation R_θ is directly applied N times. Thus, the input photon state $|1\rangle$ can be rotated to $|2\rangle$ at the end, that is,

$$(R_\theta)^N|1\rangle = R_{N\theta}|1\rangle = |2\rangle. \tag{9}$$

In summary, after N cycles, if we get $|1\rangle$, it implies the existence of the object, while $|2\rangle$ implies the absence; we can therefore unambiguously detect the presence of an object (because state $|1\rangle$ and $|2\rangle$ are orthogonal), without any photon absorption by the object. This is the essential idea of the interaction-free measurement, based on the physics of quantum Zeno effect.

B. Finite rounds and imperfect absorption

In practice, there are two problems one should consider, in implementing the interaction-free measurement. First, the number of interrogation cycles N has to be *finite*; it is also impossible to make the rotation angle arbitrarily small.

Second, the absorption of the photon by the object may not be perfect, as assumed in Eq. (4). In this paper, we consider the absorption probability to be less than unity, i.e.,

$$U_I|2\rangle = a|2\rangle + \sqrt{1-a^2}|3\rangle, \tag{10}$$

where a^2 characterizes the transparency of the object. Here a is assumed to be a non-negative real number for simplicity.

In this scenario, we can substitute a beamsplitter, the transparency of which is a^2, for the mirror in Fig. 1 to mimic the corresponding semitransparent object. This treatment is similar to Ref. [19], and other works [11,20] gave different but equivalent treatments.

C. Related works

Previous work has shown that the successful rate of IFM decreases if the object is semitransparent, compared with the opaque case [19,21,22]. The performance can be improved by increasing the interrogation cycle number N and the object can also be detected perfectly without any photon absorption when $N \to \infty$ [23,24].

However, in the literature [19,21,23,24], the initial input state is usually taken as a pure state, namely, $|1\rangle$. In the presence of an object, the successful probability

$$P_{\text{suc}} = |\langle 1|\hat{O}_{\text{IFM}}|1\rangle|^2 \tag{11}$$

is used to characterize the performance of the IFM process. Here $\hat{O}_{\text{IFM}}$ is a linear operator, but not necessarily unitary due to the possibility of photon loss. The value of P_{suc} specifies the probability that one can receive a $|1\rangle$ photon after sending a $|1\rangle$ photon at the beginning, in the presence of an object. In this case, one can confirm the presence of an object without the photon being absorbed.

To the best of our knowledge, there is no work aiming to optimize the IFM process through a search of optimal input states of the photon. In particular, the possibility of using quantum correlation to enhance the ability of channel discrimination has been achieved in the context of quantum illumination [25], which is analyzed in this paper.

D. Main results

In this paper, we provide analytic solutions to a generalized IFM model. To be specific, we focus on two main quantities to benchmark the performance of IFM, namely, (i) the loss probability P_{loss} and (ii) the error probability P_{error}, which, respectively, describe the photon loss rate and the minimum error of discriminating the object. Specifically, the minimum values of these two probabilities are investigated analytically, for any given values of the object transparency a^2 and the interrogation number N.

Our main results for unentangled input states are summarized as follows.

(1) For any finite N, there exists a unique quantum state $|\varphi_0\rangle$ minimizing P_{loss}, which approaches zero asymptotically as $N \to \infty$.

(2) There are two states $|\varphi_\pm\rangle$ that lead to $P_{\text{error}} = 0$, i.e., perfect discrimination, as long as the following inequality is fulfilled:

$$\frac{1+a}{1-a} \sin\left(\frac{\pi}{2N}\right) \leqslant 1. \tag{12}$$

(3) The photon loss rate of $|\varphi_+\rangle$ is smaller than that of $|\varphi_-\rangle$, i.e., $(P_{\text{loss}})_{|\varphi_+\rangle} < (P_{\text{loss}})_{|\varphi_-\rangle}$, which means $|\varphi_+\rangle$ is better than $|\varphi_-\rangle$ in terms of P_{loss}.

(4) For $N \to \infty$, both $|\varphi_0\rangle$ and $|\varphi_+\rangle$ approach the same state $|1\rangle$, where both $(P_{\text{loss}})_{|\varphi_0\rangle}$ and $(P_{\text{loss}})_{|\varphi_+\rangle}$ share similar asymptotic behavior $O(1/N)$.

In addition, we studied how quantum correlation of input states can facilitate the IFM process by utilizing entangled photons in the setting of quantum illumination [25]: send one photon in an entangled pair to the IFM cycle but keep the other photon. At the end, a joint POVM measurement is performed on both photons. Our main results for entangled input states are summarized as follows.

(1) The optimal state to reach the minimal P_{loss} is the product state $|\varphi_0\rangle|\phi_0\rangle$, where $|\phi_0\rangle$ is any state of the second photon, which means that entanglement can only increase P_{loss}.

(2) The two solutions $|\varphi_\pm\rangle$ expand to a family of quantum states in the larger Hilbert space. Specifically, all members of the form

$$\alpha|\varphi_+\rangle|\phi_1\rangle + \beta|\varphi_-\rangle|\phi_1^\perp\rangle \tag{13}$$

can be employed to achieve $P_{\text{error}} = 0$, where $|\phi_1\rangle$ and $|\phi_1^\perp\rangle$ are any two orthogonal states of the second photon. However, the one with the minimal P_{loss} in this family is the unentangled state $|\varphi_+\rangle|\phi_1\rangle$.

In other words, entangled photons cannot minimize P_{loss} or P_{error} better than the case with a single photon. Therefore, we conclude that entanglement cannot improve the IFM process in our setting.

The rest of the paper is organized as follows. In Sec. II, we construct a general model with the use of a quantum channel. In Sec. III, we simplify the quantum channels for pure input state. In Secs. IV and V, we study the case with an opaque object and a semitransparent object, respectively. We conclude in Sec. VI.

II. GENERAL MODEL

In this section, we present a general model of interaction-free measurement, taking into account a semitransparent object and a finite number of interrogation cycles. Later, we shall consider sending entangled photons as the input state.

First of all, the IFM process can be described as a quantum channel, which is sequentially applied N times on the input photon state, depending on the presence or absence of the object. Thus, detecting the object is equivalent to a channel discrimination problem.

In both cases, a unitary rotation operator [see Eq. (2)], in the basis $|1\rangle, |2\rangle$, and $|3\rangle$,

$$R_\theta = \begin{pmatrix} \cos\theta & -\sin\theta & 0 \\ \sin\theta & \cos\theta & 0 \\ 0 & 0 & 1 \end{pmatrix}, \tag{14}$$

is applied at each step. It can be regarded as the following channel:

$$\mathcal{E}_\theta(\rho) = R_\theta\, \rho\, R_\theta^\dagger, \tag{15}$$

where ρ is the density matrix of the input state.

If a semitransparent object is present, partial absorption can be represented by an effective quantum channel $\mathcal{E}_I$ (I stands for interaction) on the photon state (see Appendix A for detailed derivation):

$$\mathcal{E}_I(\rho) = \sum_{i=0,1} A_i \rho A_i^\dagger, \tag{16}$$

$$A_0 = |1\rangle\langle 1| + a|2\rangle\langle 2| + |3\rangle\langle 3|,$$

$$A_1 = \sqrt{1-a^2}|3\rangle\langle 2|, \tag{17}$$

where A_0 and A_1 are the Kraus operators satisfying $\sum_{i=0,1} A_i^\dagger A_i = I$.

Then the channels that describe the whole interrogation can be written down by cycling the above channels for N times as below:

$$\rho' = [\mathcal{E}_1\, \mathcal{E}_\theta]^N(\rho) = \mathcal{E}'(\rho), \tag{18}$$

$$\rho'' = [\mathcal{E}_\theta]^N(\rho) = \mathcal{E}''(\rho), \tag{19}$$

where ρ' is the output density matrix, if the object is present; ρ'' is the output density matrix for the object absence case. The corresponding overall quantum channels are denoted by $\mathcal{E}'$ and $\mathcal{E}''$, respectively.

In our setting, the photon can be absorbed when the object is present, and the photon is left in the $|3\rangle$ state, which implies that

$$P_{\text{loss}} = q\ \langle 3|\mathcal{E}'(\rho)|3\rangle, \tag{20}$$

where q is the probability for the presence of the object.

Given the object existing probability Pr(here), the error occurs when one gives the wrong judgment (see Fig. 2), i.e.,

$$\begin{aligned} P_{\text{error}} = {} & \Pr(\text{here})\Pr(\text{NO}|\text{here}) \\ & + \Pr(\text{not here})\Pr(\text{YES}|\text{not here}), \end{aligned} \tag{21}$$

where one gives the judgment NO in the presence of the object, or YES in the absence of the object.

To be specific, one sends an input photon state ρ, and receives the output photon state $\mathcal{E}'(\rho)/\mathcal{E}''(\rho)$ depending on the presence or absence of the object. Then one makes the judgment by implementing a two-value POVM measurement

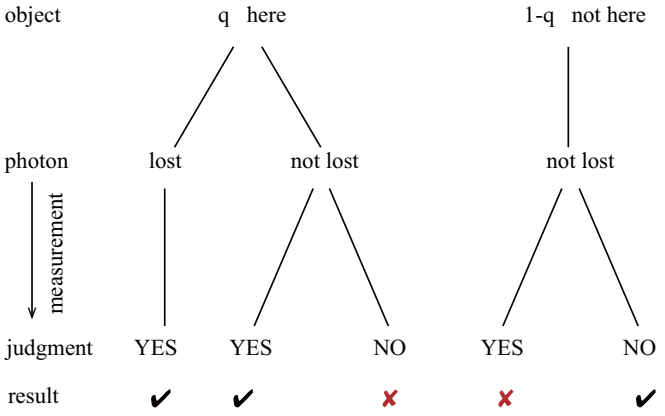

FIG. 2. Illustration for the error happening in IFM. At the end of IFM, one implements the POVM on the final output photon state, and we will make an error when giving the judgment NO (YES) in the presence (absence) of the object. The final line shows the result (right or wrong) of the judgment. And it also shows that if the photon is lost one can definitely confirm the presence of the object since the photon should not be lost in the absence of the object. Hence one can give the right judgment YES and make no error in this case.

$\{\Pi_1, \Pi_2\}$ on the final output photon. Here Π_1 and Π_2 are positive operators fulfilling $\Pi_1 + \Pi_2 = \mathbb{I}$.

The corresponding conditional probabilities in the above equation become $\Pr(\text{NO}|\text{here}) = \text{Tr}[\Pi_2 \mathcal{E}'(\rho)]$ and $\Pr(\text{YES}|\text{not here}) = \text{Tr}[\Pi_1 \mathcal{E}''(\rho)]$. Substituting them into Eq. (21), we get

$$P_{\text{error}} = q\,\text{Tr}[\Pi_2 \mathcal{E}'(\rho)] + (1-q)\text{Tr}[\Pi_1 \mathcal{E}''(\rho)]. \tag{22}$$

where we applied $\Pr(\text{here}) = q$. Actually, we can rewrite the error probability with the condition $\Pi_1 + \Pi_2 = \mathbb{I}$ as

$$P_{\text{error}} = \tfrac{1}{2}\{1 - [q\mathcal{E}'(\rho) - (1-q)\mathcal{E}''(\rho)](\Pi_1 - \Pi_2)\}. \tag{23}$$

Following Refs. [26,27], the minimal error is given by

$$P_{\text{error}} = \tfrac{1}{2}[1 - \|q\mathcal{E}'(\rho) - (1-q)\mathcal{E}''(\rho)\|], \tag{24}$$

where $||O|| \equiv \text{Tr}(\sqrt{O^\dagger O})$ denotes the trace norm of any operator O. In fact, the specific POVM reaching this minimal error is constituted by the two projectors on the positive part and negative part of the Hermitian operator $q\mathcal{E}'(\rho) - (1-q)\mathcal{E}''(\rho)$.

Note that at each cycle, if the photon detector clicks (bomb exploding in Ref. [3]), then the presence of the object can be confirmed at the middle, which makes it unnecessary to continue the following interrogation and discriminate the state at the end.

The main focus of our IFM study is to find the minima of these two probabilities P_{loss} and P_{error}, and the initial input photon states to reach them. Fortunately, with the following theorem, we can reduce the range of the input state from any density matrix ρ, say mixed or pure, to just pure state $|\varphi\rangle$ in the Hilbert space of the photon.

Theorem 1. The minima of the loss probability P_{loss} and the error probability P_{error} can be both reached by pure states.

Proof. Due to the linearity of the quantum channel, we have $P_{\text{loss}} = q\langle 3|\mathcal{E}'(\rho)|3\rangle = q\langle 3|\mathcal{E}'(\sum_i p_i\varphi_i)|3\rangle$, which implies that

$$P_{\text{loss}} = \sum_i p_i q \langle 3|\mathcal{E}'(\varphi_i)|3\rangle = \sum_i p_i P^i_{\text{loss}}, \tag{25}$$

where $\varphi_i \equiv |\varphi_i\rangle\langle\varphi_i|$ represents the density matrix of the pure state $|\varphi_i\rangle$, P^i_{loss} is the corresponding loss probability, and $\sum_i p_i\varphi_i$ is any convex decomposition of the input state ρ.

Equation (25) shows that the loss probability P_{loss} of the mixed state ρ equals to the weighted average of P^i_{loss} of the corresponding pure state. Thus there is at least one pure state φ_i with loss probability $P^i_{\text{loss}} \leqslant P_{\text{loss}}$.

On the other hand, for $P_{\text{error}} = \frac{1}{2}[1 - \|q\mathcal{E}'(\rho) - (1-q)\mathcal{E}''(\rho)\|] = \frac{1}{2}[1 - \|q\mathcal{E}'(\sum_i p_i\varphi_i) - (1-q)\mathcal{E}''(\sum_i p_i\varphi_i)\|]$, combining the convex property of the trace norm, we also have

$$\begin{aligned} P_{\text{error}} &= \frac{1}{2}\left\{1 - \left\|\sum_i p_i[q\mathcal{E}'(\varphi_i) - (1-q)\mathcal{E}''(\varphi_i)]\right\|\right\} \\ &\geqslant \sum_i p_i \left\{\frac{1}{2}[1 - \|q\mathcal{E}'(\varphi_i) - (1-q)\mathcal{E}''(\varphi_i)\|]\right\} \\ &= \sum_i p_i P^i_{\text{error}}. \end{aligned} \tag{26}$$

Similarly, one can always find a pure state in the decomposition, with $P^i_{\text{error}} \leqslant P_{\text{error}}$. Consequently, we can confine our paper to the optimal values of the two probabilities' pure states only. ■

Quantum entanglement is an essential resource for quantum communication and computation [28], and also for quantum metrology [29,30]. The efficiency of many tasks can be enhanced utilizing quantum entanglement, e.g., quantum illumination [25]. Here we also study if quantum entanglement can be employed to enhance the detection efficiency.

The idea is illustrated in Fig. 3, where a pair of entangled photons is employed as the input state. Photon A goes through the same IFM apparatus (Fig. 1) and photon B is kept at the same location during the detection period. Finally, a joint measurement is performed on the bipartite photon state.

Although physically the quantum channel is applied only on photon A, mathematically, it can be viewed as a quantum channel acting on the combined system A and B. Therefore, the argument of Theorem 1 can also be applied to this case. As a result, we only need to consider the pure state for the entangled photons. ■

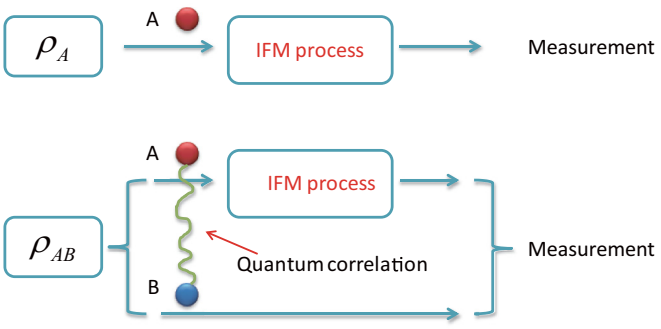

FIG. 3. The single-photon and entangled photon input IFM.

Furthermore, we show another theorem below, which describes the relation between the single-photon input case and entangled photon input about the two important probabilities P_{loss} and P_{error}.

Theorem 2. Entangled photon input is the same as single-photon input for P_{loss}, but not worse than single-photon input for P_{error}. More precisely,

$$P_{\text{loss}}(\rho_{AB}) = P_{\text{loss}}(\rho_A), \tag{27}$$

$$P_{\text{error}}(\rho_{AB}) \leqslant P_{\text{error}}(\rho_A) \tag{28}$$

where ρ_{AB} is the bipartite input state and $\rho_A = \text{Tr}_B(\rho_{AB})$.

Proof. For P_{loss}, by the definition in Eq. (20), Eq. (27) shows

$$\langle 3|\text{Tr}_B[\mathcal{E}'(\rho_{AB})]|3\rangle = \langle 3|\mathcal{E}'(\rho_A)|3\rangle, \tag{29}$$

since the partial trace operation on system B and the quantum channel on system A commute with each other.

For P_{error}, using the definition in Eq. (24), Eq. (28) is equivalent to

$$\begin{aligned}&\|q\mathcal{E}'(\rho_{AB}) - (1-q)\mathcal{E}''(\rho_{AB})\| \\ &\quad\geqslant \|q\mathcal{E}'(\rho_A) - (1-q)\mathcal{E}''(\rho_A)\|.\end{aligned} \tag{30}$$

This is because partial trace operation on B is certainly a trace-preserving operation that is contractive under the measure of trace distance (see Ref. [28] and Appendix B), i.e.,

$$\begin{aligned}&\|q\mathcal{E}'(\rho_{AB}) - (1-q)\mathcal{E}(\rho_{AB})\| \\ &\quad\geqslant \|q\text{Tr}_B[\mathcal{E}'(\rho_{AB})] - (1-q)\text{Tr}_B[\mathcal{E}(\rho_{AB})]\| \\ &\quad= \|q\mathcal{E}'(\rho_A) - (1-q)\mathcal{E}(\rho_A)\|,\end{aligned}$$

where the last line is due to partial trace on system B commuting with the quantum channel on system A. ■

III. SIMPLIFICATION OF THE QUANTUM CHANNEL FOR THE PURE STATE

From Theorem 1, we just need to focus on the pure input state scenario for the optimal solutions. The quantum channels defined in Sec. II can be simplified when the input state is pure.

First, let us consider a general input state, $|\varphi\rangle = \alpha|1\rangle + \beta|2\rangle$. In the presence of the object scenario, since the IFM process halts in the probability subspace where the photon decays to the loss state $|3\rangle$, we just need to consider the probability subspace where the photon is not absorbed, and the corresponding un-normalized state (due to absorption) is denoted as $|\varphi'\rangle$.

The final photon state, in the presence of the object, is of the following form:

$$\rho' = |\varphi'\rangle\langle\varphi'| + (1 - \langle\varphi'|\varphi'\rangle)|3\rangle\langle 3|. \tag{31}$$

The quantum channels can be replaced by the corresponding transforming matrix for the pure state in the $|1\rangle,|2\rangle$ basis as

$$M'|\varphi\rangle = |\varphi'\rangle, \tag{32}$$

where

$$M' \equiv \left[\begin{pmatrix}1 & 0\\ 0 & a\end{pmatrix}\begin{pmatrix}\cos\theta & -\sin\theta\\ \sin\theta & \cos\theta\end{pmatrix}\right]^N. \tag{33}$$

In the absence of the object, the final output photon state is given by

$$M''|\varphi\rangle = |\varphi''\rangle, \tag{34}$$

where

$$M'' \equiv \left[\begin{pmatrix}\cos\theta & -\sin\theta\\ \sin\theta & \cos\theta\end{pmatrix}\right]^N = \begin{pmatrix}0 & -1\\ 1 & 0\end{pmatrix}. \tag{35}$$

Here, Eqs. (32) and (34) give the relations between $|\varphi\rangle = \alpha|1\rangle + \beta|2\rangle$ and $|\varphi'\rangle, |\varphi''\rangle$. Equation (34) is just the unitary transformation generated by the rotation operation R_θ [Eq. (14)] on the photon state in each cycle, and we obtain the final state by iterating it N times. However, Eq. (32) is not a unitary transformation, as it includes the effect of irreversible photon loss.

Consequently, $P_{\text{loss}} = q\ \langle 3|\rho'|3\rangle$ is given by

$$\begin{aligned}P_{\text{loss}} &= q\ \langle 3||\varphi'\rangle\langle\varphi'| + (1 - \langle\varphi'|\varphi'\rangle)|3\rangle\langle 3||3\rangle \\ &= q\ (1 - \langle\varphi'|\varphi'\rangle).\end{aligned} \tag{36}$$

Now, since $\langle 3|\varphi''\rangle = 0$, with the definition of P_{error} in Eq. (24) we have

$$P_{\text{error}} = \tfrac{1}{2}\{1 - P_{\text{loss}} - \|q|\varphi'\rangle\langle\varphi'| - (1-q)|\varphi''\rangle\langle\varphi''|\|\}. \tag{37}$$

On the other hand, the general form of the entangled photon input state can be written as

$$|\varphi_e\rangle \equiv \alpha|1\rangle|\phi_1\rangle + \beta|2\rangle|\phi_2\rangle, \tag{38}$$

where $|\phi_1\rangle$, $|\phi_2\rangle$ are some pure states of the ancillary photon B.

Now the transfer matrices in Eqs. (32) and (34) should be applied on photon A of the entangled input state, that is,

$$\begin{aligned}M' \otimes \mathbb{I}|\varphi_e\rangle &= |\varphi'_e\rangle, \\ M'' \otimes \mathbb{I}|\varphi_e\rangle &= |\varphi''_e\rangle.\end{aligned} \tag{39}$$

If photon A has been transformed to the loss state $|3\rangle$, it accounts for photon loss no matter the state of photon B. In this case, one can confirm the presence of the object without detection error. Thus, the final expressions of P_{loss} and P_{error} in Eqs. (36) and (37) are also suitable for the entangled input, if $|\varphi'_e\rangle$ and $|\varphi''_e\rangle$ are employed.

In the following, the single-photon and entangled photon input states we consider are $|\varphi_s\rangle = \alpha|1\rangle + \beta|2\rangle$ and $|\varphi_e\rangle = \alpha|1\rangle|\phi_1\rangle + \beta|2\rangle|\phi_2\rangle$ type, respectively. And we employ $|\varphi\rangle$ to represent both types of input state for simplicity.

At the end of this section, we show another theorem below, describing the condition where the error probability P_{error} can reach zero, for both single-photon and entangled photon input. In other words, we can decide whether there is an object without any error.

Theorem 3. For any pure entangled state, $P_{\text{error}} = 0$ iff $\langle\varphi''|\varphi'\rangle = 0$.

Before we prove Theorem 3, let us show a lemma first, which is useful to our proof.

Lemma 1. Given two pure quantum states, $|\psi_1\rangle$ and $|\psi_2\rangle$, and a positive real number p, the following equality holds:

$$\|p|\psi_1\rangle\langle\psi_1| - |\psi_2\rangle\langle\psi_2|\| = \sqrt{(p+1)^2 - 4p|\langle\psi_1|\psi_2\rangle|^2}. \tag{40}$$

We leave the proof of Lemma 1 to Appendix C.

Proof. With the definition in Eq. (37), P_{error} is

$$\begin{aligned} P_{\text{error}} &= \frac{1}{2}\{1 - P_{\text{loss}} - \||q|\varphi'\rangle\langle\varphi'| - (1-q)|\varphi''\rangle\langle\varphi''|\|\} \\ &= \frac{1}{2}\{q\langle\varphi'|\varphi'\rangle + 1 - q - \||q|\varphi'\rangle\langle\varphi'| \\ &\quad - (1-q)|\varphi''\rangle\langle\varphi''|\|\} \\ &= \frac{1}{2}\left\{q\langle\varphi'|\varphi'\rangle + 1 - q \right. \\ &\quad \left. - (1-q)\left\|\frac{q\langle\varphi'|\varphi'\rangle}{1-q}\frac{|\varphi'\rangle\langle\varphi'|}{\langle\varphi'|\varphi'\rangle} - |\varphi''\rangle\langle\varphi''|\right\|\right\} \\ &= \frac{1}{2}\{q\langle\varphi'|\varphi'\rangle + 1 - q \\ &\quad - \sqrt{(q\langle\varphi'|\varphi'\rangle + 1 - q)^2 - 4q(1-q)|\langle\varphi''|\varphi'\rangle|^2}\}, \end{aligned} \tag{41}$$

where in the second line we apply the definition of P_{loss} in Eq. (36) and in the last line we employ Lemma 1, by substituting $\frac{|\varphi'\rangle}{\sqrt{\langle\varphi'|\varphi'\rangle}}$, $|\varphi''\rangle$ for $|\psi_1\rangle$, $|\psi_2\rangle$ and $\frac{q\langle\varphi'|\varphi'\rangle}{1-q}$ for p. Then, let us observe the last line in Eq. (41): the second part in the square root, i.e., $4q(1-q)|\langle\varphi''|\varphi'\rangle|^2$, is non-negative, so $P_{\text{error}} = 0$ iff $\langle\varphi''|\varphi'\rangle = 0$. ■

IV. OPAQUE OBJECT SCENARIO

We study IFM of an opaque object with finite interrogation cycle N in this section. Our task is to use the model simplified in Sec. III to find the minimal values of the two important probabilities P_{loss} and P_{error}, and the corresponding states to reach them. When the object is opaque, i.e., $a = 0$, Eq. (32) becomes

$$\begin{pmatrix} \cos^N\theta & -\sin\theta\cos^{N-1}\theta \\ 0 & 0 \end{pmatrix}|\varphi\rangle = |\varphi'\rangle. \tag{42}$$

A. With single-photon input

First, let us focus on the loss probability P_{loss}. Setting the input state as $|\varphi\rangle = \alpha|1\rangle + \beta|2\rangle$ and using Eqs. (36) and (42), we get

$$|\varphi'\rangle = \cos^{N-1}\theta(\alpha\cos\theta - \beta\sin\theta)|1\rangle, \tag{43}$$

and, hence,

$$\begin{aligned} P_{\text{loss}} &= q(1 - |\cos^{N-1}\theta(\alpha\cos\theta - \beta\sin\theta)|^2) \\ &\geqslant q(1 - \cos^{2(N-1)}\theta), \end{aligned} \tag{44}$$

where the inequality in the second line of Eq. (44) is due to the fact that the absolute value of the inner product for the two vectors $(\cos\theta, -\sin\theta)^T$ and $(\alpha,\beta)^T$ is not larger than 1. Furthermore, the minimum can be reached by the state $|\varphi_a\rangle = \cos\theta|1\rangle - \sin\theta|2\rangle$ (up to a global phase).

Then we study the error probability P_{error}. By calculating the value of $\langle\varphi''|\varphi'\rangle$, we can check whether there are input states satisfying the condition stated in Theorem 3 and letting P_{error} reach zero. With the help of Eqs. (34) and (43), we have

$$|\varphi''\rangle = -\beta|1\rangle + \alpha|2\rangle, \tag{45}$$

which means that

$$\langle\varphi''|\varphi'\rangle = -\beta^*\cos^{N-1}\theta(\alpha\cos\theta - \beta\sin\theta). \tag{46}$$

We found two states satisfying the condition $\langle\varphi''|\varphi'\rangle = 0$. The first one is $|\varphi_b\rangle = |1\rangle$, and the second one is $|\varphi_c\rangle = \sin\theta|1\rangle + \cos\theta|2\rangle$. That is, one can realize zero error in IFM with these two states. However, from Eq. (36), we found that

$$P_{\text{loss}}(|\varphi_b\rangle) = q(1 - \cos^{2N}\theta), \tag{47}$$

but

$$P_{\text{loss}}(|\varphi_c\rangle) = q, \tag{48}$$

which is independent of N.

Thus, it is necessary to compare the loss probability P_{loss} of $|\varphi_b\rangle$, $|\varphi_c\rangle$. And the P_{loss} values of the two states are $q(1 - \cos^{2N}\theta)$ and q, respectively, by the definition of Eq. (36). This indicates that the first state is better than the second one considering P_{loss}, since, when N is large enough,

$$q(1 - \cos^{2N}\theta) \simeq q\frac{\pi^2}{4N} \ll q. \tag{49}$$

And note that the P_{loss} of $|\varphi_b\rangle$ approaches zero as $N \to \infty$ [4,6]. For the second state $|\varphi_c\rangle$, the photon is always lost if the object is there; this is the reason why $|\varphi_c\rangle$ can detect the object without any error. But it is useless since it violates the principle of IFM, i.e., detecting the object with as small as possible photon loss probability.

B. With entangled photon input

Here we study the effect of quantum correlation to IFM in the opaque object scenario. So we set the initial input state as the general form

$$|\varphi\rangle = \alpha|1\rangle|\phi_1\rangle + \beta|2\rangle|\phi_2\rangle, \tag{50}$$

where $|\phi_1\rangle$ and $|\phi_2\rangle$ are any pure states of the photon B part and α and β are non-negative real numbers (one can always remove the phase information in α and β to the states $|\phi_1\rangle$ and $|\phi_2\rangle$ of the photon B part to obtain this form).

As mentioned earlier, the equations utilized in the single-photon input case can also be used in this entangled photon input case. And we should do the transforming matrix operations on the photon A part and evaluate the two probabilities P_{loss} and P_{error} in the same way as in Sec. IV A. For P_{loss}, using Eq. (42), we have

$$|\varphi'\rangle = \cos^{N-1}\theta|1\rangle(\alpha\cos\theta|\phi_1\rangle - \beta\sin\theta|\phi_2\rangle), \tag{51}$$

and with the help of Eq. (36) the loss probability is

$$\begin{aligned} P_{\text{loss}} &= q[1 - |\cos^{N-1}\theta|1\rangle(\alpha\cos\theta|\phi_1\rangle - \beta\sin\theta|\phi_2\rangle)|^2] \\ &= q\{1 - \cos^{2(N-1)}\theta[\alpha^2\cos^2\theta + \beta^2\sin^2\theta \\ &\quad - 2\alpha\beta\cos\theta\sin\theta\,\text{Re}(\langle\phi_1||\phi_2\rangle)]\} \\ &\geqslant q[1 - \cos^{2(N-1)}\theta(\alpha\cos\theta + \beta\sin\theta)^2] \\ &\geqslant q[1 - \cos^{2(N-1)}\theta]. \end{aligned} \tag{52}$$

Here the first inequality is saturated when $\langle\phi_1||\phi_2\rangle = -1$, and the second inequality is saturated when $\alpha = \cos\theta$ and

$\beta = \sin\theta$. Thus, the minimum of P_{loss} can be reached by the following product state (i.e., no entanglement):

$$|\varphi_a^*\rangle = (\cos\theta|1\rangle - \sin\theta|2\rangle)|\phi_1\rangle, \tag{53}$$

where we use the superscript $*$ to label the bipartite state.

For P_{error}, with Eq. (43), we can obtain the output state in the absence of the object as

$$|\varphi''\rangle = \alpha|2\rangle|\phi_1\rangle - \beta|1\rangle|\phi_2\rangle, \tag{54}$$

and, applying Eq. (51), the value of $\langle\varphi''|\varphi'\rangle$ shows the following form:

$$\langle\varphi''|\varphi'\rangle = (-\alpha\beta\cos\theta\langle\phi_2|\phi_1\rangle + \beta^2\sin\theta)\cos^{N-1}\theta. \tag{55}$$

From Eq. (55), we can get a family of the solutions for $\langle\varphi''|\varphi'\rangle = 0$ which satisfies

$$\frac{\beta\sin\theta}{\alpha\cos\theta} = \langle\phi_2|\phi_1\rangle. \tag{56}$$

The two solutions in the single-photon input case are both included in Eq. (56). They are the states $|\varphi_b^*\rangle = |1\rangle|\phi_1\rangle$ and $|\varphi_c^*\rangle = (\sin\theta|1\rangle + \cos\theta|2\rangle)|\phi_1\rangle$. Now we shall check which one is the best state in this family via considering P_{loss}. With Eqs. (36) and (56),

$$P_{\text{loss}} = q[1 - \cos\theta^{2(N-1)}(\alpha^2\cos^2\theta - \beta^2\sin^2\theta)]. \tag{57}$$

It is clear that $|\varphi_b^*\rangle = |1\rangle|\phi_1\rangle$ reaches the minimum $q(1 - \cos^{2N}\theta)$ in this family, which is equivalent to $|\varphi_b\rangle$ in the single-photon input case.

From Secs. IV A and IV B, we conclude that the entangled photon input state makes no enhancement to the optimization for the two important probabilities P_{loss} and P_{error}, respectively, compared with the single-photon input state. The states which reach the minima are the same in some sense in these two cases. In addition, the state $|1\rangle$ is the optimal state that makes P_{loss} and P_{error} both reach zero when $N \to \infty$.

V. SEMITRANSPARENT OBJECT SCENARIO

In this section, we go further for the general scenario. In practical application of IFM, the object is always semitransparent, i.e., partially absorbing the photon. Thus, here we study the minimal P_{loss} and P_{error}, and the states to reach them also in this semitransparent object scenario, just like in the opaque object scenario. In addition, the effect of quantum entanglement is also investigated.

A. Simplification of the transforming matrix

The major difficulty to study the general scenario is to simplify the matrix $M' \equiv (C_0)^N$, where

$$C_0 = \begin{pmatrix} 1 & 0 \\ 0 & a \end{pmatrix}\begin{pmatrix} \cos\theta & -\sin\theta \\ \sin\theta & \cos\theta \end{pmatrix}, \tag{58}$$

in Eq. (32). First, we can represent the matrix in one interrogation cycle with Pauli matrices as

$$C_0 = \frac{(1-a)\cos\theta}{2}\sigma_z - \frac{i(1+a)\sin\theta}{2}\sigma_y - \frac{(1-a)\sin\theta}{2}\sigma_x + \frac{(1+a)\cos\theta}{2}I. \tag{59}$$

Then, we change the basis by applying a unitary transformation $U = e^{-i\frac{\sigma_y}{2}\theta}$ and obtain

$$\begin{aligned} C_1 &= UC_0U^\dagger, \\ &= \frac{(1-a)}{2}\sigma_z - \frac{i(1+a)\sin\theta}{2}\sigma_y + \frac{(1+a)\cos\theta}{2}I \\ &= \frac{(1-a)}{2}(\sigma_z - ik_1\sigma_y + k_2 I), \end{aligned} \tag{60}$$

where we defined

$$\begin{aligned} k_1 &\equiv \frac{(1+a)\sin\theta}{1-a}, \\ k_2 &\equiv \frac{(1+a)\cos\theta}{1-a}, \end{aligned} \tag{61}$$

which are both positive numbers.

The power N of the matrix C_1, labeled by

$$C \equiv (C_1)^N, \tag{62}$$

can be calculated by expanding the binomial with the help of the equality

$$(\sigma_z - ik_1\sigma_y)^2 = \left(1 - k_1^2\right)I, \tag{63}$$

which is the result of the anticommutation relation $\{\sigma_z,\sigma_y\} = 0$:

$$\begin{aligned} C = C_1^N &= \left(\frac{1-a}{2}\right)^N [(\sigma_z - ik_1\sigma_y) + k_2 I)]^N \\ &= \left(\frac{1-a}{2}\right)^N \Bigg[\sum_{k\in\text{odd}}\binom{N}{k}\left(1-k_1^2\right)^{\frac{k-1}{2}}k_2^{N-k}(\sigma_z - ik_1\sigma_y) \\ &\quad + \sum_{k\in\text{even}}\binom{N}{k}\left(1-k_1^2\right)^{\frac{k}{2}}k_2^{N-k}I\Bigg] \\ &= \left(\frac{1-a}{2}\right)^N [f_1(\sigma_z - ik_1\sigma_y) + f_2 I], \end{aligned} \tag{64}$$

where we substitute f_1 and f_2 for the summations before the operators $(\sigma_z - ik_1\sigma_y)$ and I, respectively. In fact, f_1 and f_2 are related to the summations of the even and odd terms in the corresponding binomial.

Thus, we define Σ_1 and Σ_2 as below, which are sums of the odd and even terms of the corresponding binomial. When $k_1 \leqslant 1$,

$$\begin{aligned} \Sigma_1 &= \frac{\left(\sqrt{1-k_1^2}+k_2\right)^N - \left(-\sqrt{1-k_1^2}+k_2\right)^N}{2} \\ \Sigma_2 &= \frac{\left(\sqrt{1-k_1^2}+k_2\right)^N + \left(-\sqrt{1-k_1^2}+k_2\right)^N}{2}; \end{aligned} \tag{65}$$

when $k_1 > 1$,

$$\begin{aligned} \Sigma_1 &= \frac{\left(i\sqrt{k_1^2-1}+k_2\right)^N - \left(-i\sqrt{k_1^2-1}+k_2\right)^N}{2} \\ \Sigma_2 &= \frac{\left(i\sqrt{k_1^2-1}+k_2\right)^N + \left(-i\sqrt{k_1^2-1}+k_2\right)^N}{2}. \end{aligned} \tag{66}$$

Then we can obtain the expressions for f_1 and f_2 in Eq. (64) with Σ_1 and Σ_2, when $k_1 \leqslant 1$:

$$f_1 = \frac{\Sigma_1}{\sqrt{1-k_1^2}}$$
$$f_2 = \Sigma_2; \tag{67}$$

when $k_1 > 1$,

$$f_1 = \frac{\Sigma_1}{i\sqrt{k_1^2-1}}$$
$$f_2 = \Sigma_2. \tag{68}$$

The insight of the above result is that the eigenstates of C_1 and C should be the same and the eigenvalues from C are just power N of the ones from C_1. So the structures of Eqs. (60) and (64) are also the same, the linear combination of $(\sigma_z - ik_1\sigma_y)$ and I. Especially, $(\sigma_z - ik_1\sigma_y)$ determines the eigenstates, and the eigenvalues of it are $\pm\sqrt{1-k_1^2}$. That is why we have the formulas like Eqs. (65)–(68). Clearly, f_1 and f_2 are functions of a and θ and we show that they are both real positive numbers in the following theorem.

Theorem 4. f_1 and f_2 are both real positive numbers no matter what value k_1 is.

Proof. When $k_1 \leqslant 1$, Σ_1 and Σ_2 are the sum of odd and even terms of $(\sqrt{1-k_1^2}+k_2)^N$, respectively. It is obvious that f_1 and f_2 are both real positive numbers. When $k_1 > 1$, Σ_1 and Σ_2 are the imaginary and real part of $(i\sqrt{k_1^2-1}+k_2)^N$. We just need to check which quadrant this complex number locates in. Because $\frac{\sqrt{k_1^2-1}}{k_2} \leqslant \frac{k1}{k2} = \tan\theta$ and $N\theta = \frac{\pi}{2}$, we know it locates in the first quadrant. Then f_1 and f_2 are also real positive numbers in this case by the definition Eq. (68). ■

B. P_{loss} study with single-photon and entangled photon input states

With the knowledge of Sec. V A, now we can get the loss probability P_{loss} in the new basis by the definition in Eq. (36) as

$$\begin{aligned} P_{\text{loss}} &= q(1-\langle\varphi'|\varphi'\rangle) \\ &= q(1-\langle\varphi|C^\dagger C|\varphi\rangle) \\ &= q[1-\text{Tr}_{AB}(C^\dagger C|\varphi\rangle\langle\varphi|)] \\ &= q[1-\text{Tr}_A(C^\dagger C\rho_A)], \end{aligned} \tag{69}$$

where in the final line we trace out the photon B part since the transforming matrix C just operates on photon A. Equation (69) reminds us that entangled photon input state $|\varphi_{AB}\rangle$ behaves the same as $\text{Tr}_B(\varphi_{AB}) = \rho_A$ for P_{loss}, as shown in Theorem 2. Especially, if one reaches the minimum of P_{loss} with single-photon input state $|\varphi_A\rangle$, one can surely find any pure state like $|\varphi_A\rangle|\phi_B\rangle$ to reach the same minimal value. Hence we just need to study P_{loss} in the single-photon input case.

Thus $\langle\varphi|C^\dagger C|\varphi\rangle$ in Eq. (69) should be maximized only for the single-photon input state, and $C^\dagger C$ can be expanded as

$$C^\dagger C = \left(\frac{1-a}{2}\right)^{2N}\left[f_1^2(1+k_1^2)+f_2^2\right]I + 2f_1(f_2\sigma_z - f_1k_1\sigma_x). \tag{70}$$

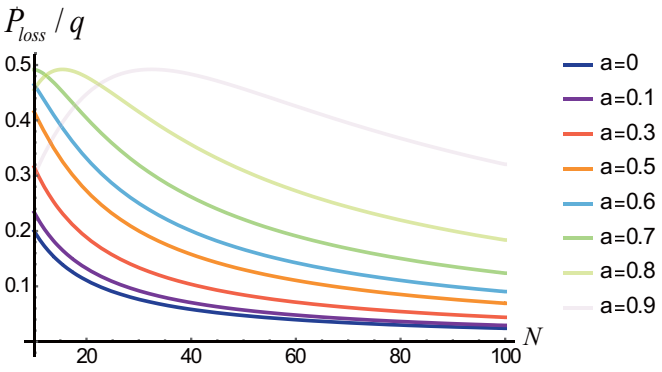

FIG. 4. $(P_{\text{loss}}/q)_{\text{min}}$ vs the interrogation cycle N for different transparency a^2.

It is the same as to find the larger eigenvalue for a single spin Hamiltonian. Thus, no matter what value k_1 is, it is not hard to obtain the minimal P_{loss}:

$$(P_{\text{loss}})_{\text{min}} = q\left[1-\left(\frac{1-a}{2}\right)^{2N}\left(f_1+\sqrt{f_2^2+f_1^2k_1^2}\right)^2\right]. \tag{71}$$

Utilizing Eq. (71), the relation between the normalized photon loss rate $(P_{\text{loss}}/q)_{\text{min}}$ and the interrogation cycle N for different transparency a^2 is exhibited in Fig. 4. This figure shows that when N is large enough $(P_{\text{loss}}/q)_{\text{min}}$ decreases with the increasing of N no matter what value a is. Generally speaking, $(P_{\text{loss}}/q)_{\text{min}}$ of small a is always less than that of large a for a fixed large enough N. However, $(P_{\text{loss}}/q)_{\text{min}}$ can increase and then decrease for large enough a with the increasing of N. Via numerical analysis, we find that the maximum of the curve for a given large a can be obtained at N', which is slightly larger than the one determined by the equation

$$k_1 = \frac{1+a}{1-a}\sin\left(\frac{\pi}{2N}\right) = 1, \tag{72}$$

as shown in Fig. 5.

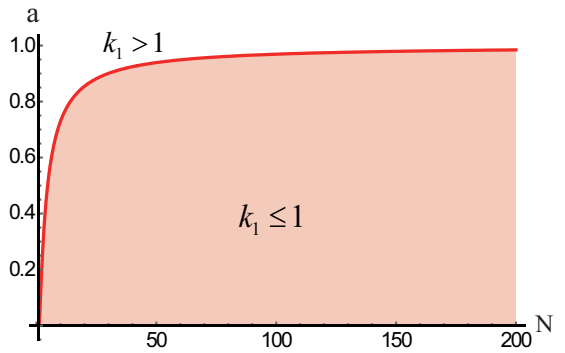

FIG. 5. Red envelope (gray) curve: Transparency a vs interrogation cycle N determined by $k_1 = \frac{1+a}{1-a}\sin(\frac{\pi}{2N}) = 1$. The shadow (light gray) region indicates the parameter domain where we can reach $P_{\text{error}} = 0$.

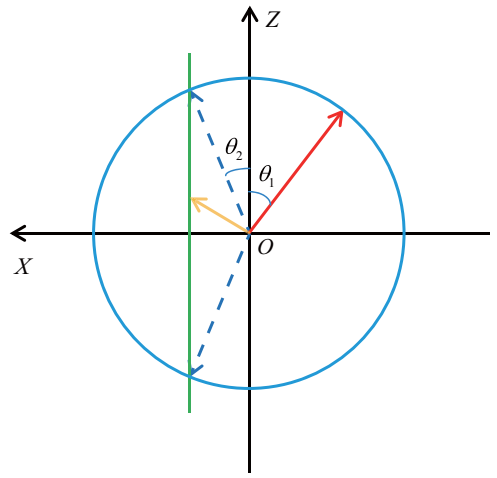

FIG. 6. The positions of the states on the Bloch sphere that reach the minimal P_{loss} and P_{error} in the new basis. The red (solid) arrow represents the state $|\varphi_0\rangle\langle\varphi_0|$ which reaches the minimal P_{loss}. The two blue (dashed) arrows represent $|\varphi_\pm\rangle\langle\varphi_\pm|$. Any mixed state on the green (vertical) line, the connection between the end of the two blue (dashed) arrows, satisfies $\text{Tr}_A(D^\dagger C\rho_A) = 0$. The yellow (light gray) arrow represents one of these mixed states, and its purification is an entangled photon input state $\alpha|\varphi_+\rangle|\phi_1\rangle + \beta|\varphi_-\rangle|\phi_1^\perp\rangle$ making $P_{\text{error}} = 0$.

The state reaching the minimum of P_{loss}, named $|\varphi_0\rangle$, is just the eigenstate of $C^\dagger C$ with larger eigenvalue. $|\varphi_0\rangle\langle\varphi_0|$ is on the XZ plane of the Bloch sphere. And the angle between $|\varphi_0\rangle\langle\varphi_0|$ and the Z axis is $\theta_1 = \arctan(\frac{f_1 k_1}{f_2})$ (see Fig. 6). The corresponding vector $U^\dagger|\varphi_0\rangle$ is the one which reaches the minimal P_{loss} in the old basis. And it is not hard to find $U^\dagger|\varphi_0\rangle = |\varphi_a\rangle$ when the transparency $a^2 = 0$, i.e., the opaque object scenario.

C. P_{error} study with single-photon and entangled photon input states

Here, we derive the error probability P_{error} of IFM in both single-photon and entangled photon input cases.

For convenience, we label the unitary transformation in Eq. (34) by D, as the object is absent:

$$D = \begin{pmatrix} 0 & -1 \\ 1 & 0 \end{pmatrix} = -i\sigma_y. \tag{73}$$

In Theorem 3, we have showed that P_{error} can reach zero iff $\langle\varphi''|\varphi'\rangle = 0$, no matter which type the input state is. By definition, we get $\langle\varphi''|\varphi'\rangle$ in the new basis as

$$\begin{aligned}\langle\varphi''|\varphi'\rangle &= \langle\varphi|UD^\dagger U^\dagger C|\varphi\rangle \\ &= \langle\varphi|D^\dagger C|\varphi\rangle \\ &= \text{Tr}_{AB}(D^\dagger C|\varphi\rangle\langle\varphi|) \\ &= \text{Tr}_A(D^\dagger C\rho_A)\end{aligned} \tag{74}$$

where $D \to UDU^\dagger$ in the new basis. In the second line, we use the fact that U commutes with $D^\dagger$. The third line is due to the fact that $D^\dagger$ and C only operate on the photon A part.

From the definition of D and C, we have $D^\dagger C$:

$$D^\dagger C = \left(\frac{1-a}{2}\right)^N [f_1 k_1 I + (if_2\sigma_y - f_1\sigma_x)]. \tag{75}$$

In the meantime, ρ_A has the following Bloch sphere representation:

$$\rho_A = \tfrac{1}{2}(I + \vec{r}\cdot\vec{\sigma}). \tag{76}$$

Then Eq. (74) becomes $\langle\varphi''|\varphi'\rangle = (\frac{1-a}{2})^N(f_1 k_1 - f_1 r_x + if_2 r_y)$ with the fact that the trace of the Pauli matrix is zero. In order to make $P_{\text{error}} = 0$, we should let $r_x = k_1$ and $r_y = 0$.

When $k_1 \leqslant 1$, there are two pure state solutions $\rho_A = |\varphi_\pm\rangle\langle\varphi_\pm| = \frac{1}{2}(I + k_1\sigma_x \pm \sqrt{1-k_1^2}\sigma_z)$ of photon A. The angle between each pure solution $|\varphi_\pm\rangle\langle\varphi_\pm|$ and the Z axis is $\theta_2 = \arctan(\frac{k_1}{\sqrt{1-k_1^2}})$ on the Bloch sphere (see Fig. 5). And it is straightforward to see that any convex mixing of the two pure solutions can also lead to $\text{Tr}_A(D^\dagger C\rho_A) = 0$. Therefore, in the bipartite case, the solution to $P_{\text{error}} = 0$ is $\alpha|\varphi_+\rangle|\phi_1\rangle + \beta|\varphi_-\rangle|\phi_1^\perp\rangle$, where $\langle\phi_1^\perp|\phi_1\rangle = 0$ and α and β are two arbitrary state coefficients. Like in the $a = 0$ scenario, we have a family of best states which reach $P_{\text{error}} = 0$ in the entangled photon input case.

Furthermore, we aim to find the solution that minimizes the photon loss rate P_{loss} given in Eq. (69) in this family. Combining the solution to $P_{\text{error}} = 0$, we can show that the optimal state in this family is $|\varphi_+\rangle\langle\varphi_+| = \frac{1}{2}(I + k_1\sigma_x + \sqrt{1-k_1^2}\sigma_z)$ with the minimal P_{loss} value

$$(P_{\text{loss}})_{|\varphi_+\rangle} = q\left[1 - \left(\frac{1-a}{2}\right)^{2N}\left(f_1\sqrt{1-k_1^2} + f_2\right)^2\right], \tag{77}$$

which means the entangled photon input state does no good to P_{error} in this k_1 regime.

When $k_1 > 1$, there is no solution to $\langle\varphi''|\varphi'\rangle = 0$ or equivalently $P_{\text{error}} = 0$. Nevertheless, we can still analyze the nonzero minimum of P_{error}. Using Eqs. (41), (69), and (74), we have the general expression of P_{error}:

$$\begin{aligned}&P_{\text{error}} \\ &= \frac{1}{2}\{q\,\text{Tr}[C^\dagger C\rho_A] + (1-q) \\ &\quad - \sqrt{(q\,\text{Tr}[C^\dagger C\rho_A]+1-q)^2 - 4q(1-q)|\text{Tr}[D^\dagger C\rho_A]|^2}\},\end{aligned} \tag{78}$$

which is suitable no matter what value k_1 is. This indicates that $|\varphi_{AB}\rangle$ appears in the form $Tr_B(\varphi_{AB}) = \rho_A$ for P_{error} in all k_1 regimes. It is crucial to emphasize that the expression for P_{error} of Eq. (78) is suitable for any pure states, single-photon or entangled photon input, but not for mixed state ρ_A, because of our pure state prerequisite. Moreover, we find the entangled photon input state cannot enhance the performance on P_{error} for any values of k_1, compared with the single-photon input state, i.e., the minimum of Eq. (78) should be reached by pure state $\rho_A = |\varphi_A\rangle\langle\varphi_A|$. The detailed discussion about the effect of quantum correlation to P_{error} is given in Appendix D.

D. $N \to \infty$ behavior

In the above subsections, we have systematically analysed the general IFM model of the semitransparent object with finite interrogation cycle. Now, in this part, we study the asymptotic behavior of the relevant quantities when the interrogation cycle $N \to \infty$. The behavior of the minimal values of P_{loss} and P_{error} and the initial input states reaching them are investigated in the $N \to \infty$ condition.

When the interrogation cycle $N \to \infty, k_1 = \frac{1+a}{1-a}\sin(\frac{\pi}{2N}) \to 0 < 1$ for any fixed a. Therefore we always have the state $|\varphi_+\rangle$ to reach $P_{\text{error}} = 0$. First we consider the asymptotic behavior of $(P_{\text{loss}})_{|\varphi_+\rangle}$, described by Eq. (77). With the help of Eqs. (65) and (67) and the definitions of k_1 and k_2 [Eq. (61)], we have

$$\begin{aligned}
&\left(\frac{1-a}{2}\right)^{2N}\left(f_1\sqrt{1-k_1^2}+f_2\right)^2 \\
&= \left(\frac{1-a}{2}\right)^{2N}(\Sigma_1+\Sigma_2)^2 \\
&= \left[\frac{1-a}{2}\left(k_2+\sqrt{1-k_1^2}\right)\right]^{2N} \\
&= \left[\frac{(1+a)\cos\theta+\sqrt{(1-a)^2-(1+a)^2\sin^2\theta}}{2}\right]^{2N} \\
&\simeq \left[1-\frac{1+a}{1-a}\frac{\pi^2}{8N^2}+O\left(\frac{1}{N^4}\right)\right]^{2N} \\
&\simeq 1-\frac{1+a}{1-a}\frac{\pi^2}{4N}+O\left(\frac{1}{N^3}\right),
\end{aligned} \tag{79}$$

where we use the fact that $\cos\theta = 1-\frac{\theta^2}{2}+O(\theta^4)$, $\sin\theta = \theta - O(\theta^3)$, and $\theta = \frac{\pi}{2N}$. Then the asymptotic expression of Eq. (77) is

$$(P_{\text{loss}})^{N\to\infty}_{|\varphi_+\rangle} \simeq q\left[\frac{1+a}{1-a}\frac{\pi^2}{4N}-O\left(\frac{1}{N^3}\right)\right]. \tag{80}$$

Clearly, whatever the value of a is, $(P_{\text{loss}})_{|\varphi_+\rangle}$ goes to zero for sufficiently large N.

Furthermore, we aim to consider the asymptotic behavior of the minimum of P_{loss}, in Eq. (71). Utilizing a similar approximation technique as for $(P_{\text{loss}})_{|\varphi_+\rangle}$, we have

$$(P_{\text{loss}})^{N\to\infty}_{\text{min}} \simeq q\left[\frac{1+a}{1-a}\frac{\pi^2}{4N}-O\left(\frac{1}{N^2}\right)\right]. \tag{81}$$

The detailed derivation is given in Appendix E. In addition, the asymptotic behaviors of $(P_{\text{loss}})_{|\varphi_+\rangle}/q$ and $(P_{\text{loss}})_{\text{min}}/q$ have been plotted in Fig. 7.

When $N \to \infty, \theta_1$ and θ_2, relating to the initial input states $|\varphi_0\rangle$ and $|\varphi_+\rangle$, both go to zero (see Fig. 7). And the unitary $U = e^{-i\frac{\sigma_y}{2}\theta}$ of changing basis goes to identity. Hence, the corresponding vector $U^\dagger|\varphi_0\rangle$ which reaches $(P_{\text{loss}})_{\text{min}}$ and $U^\dagger|\varphi_+\rangle$ which reaches the minimum of P_{loss} but keeps $P_{\text{error}} = 0$ in the old basis go to the same vector $(1,0)^T$, i.e., $|1\rangle$ in our system. That is to say, as $N \to \infty$, we can use $|1\rangle$ to realize $P_{\text{loss}} = P_{\text{error}} = 0$ asymptotically, perfectly detecting the object without photon loss even if the object is a semitransparent one.

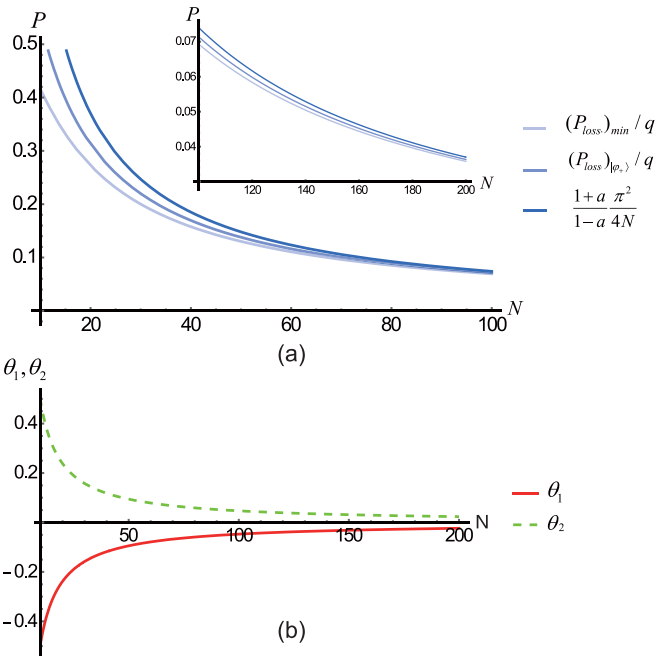

FIG. 7. All the graphs are plotted at $a = 0.5$. (a) The asymptotic behaviors of $(P_{\text{loss}})_{|\varphi_+\rangle}/q$,$(P_{\text{loss}})_{\text{min}}/q$ as $N \to \infty$. $(P_{\text{loss}})_{|\varphi_+\rangle}/q$ is always above $(P_{\text{loss}})_{\text{min}}/q$. The main term of the asymptotic expressions in Eqs. (80) and (81), i.e., $\frac{1+a}{1-a}\frac{\pi^2}{4N}$, is also shown in the plot. Inset: N ranges from 100 to 200. All three expressions go to zero asymptotically when $N \to \infty$. (b) The asymptotic behavior of θ_1 (solid) and θ_2 (dashed). We use the negative sign for θ_1 because it is located at the negative x-axis side, as shown in Fig. 6.

VI. CONCLUSION AND OUTLOOK

In conclusion, with the help of quantum channel theory, we build the general model of quantum-Zeno-like IFM, where the object to be detected is semitransparent and the number of interrogation cycles is finite. Two important probabilities named P_{loss} and P_{error} are proposed to describe the photon loss rate and the error of discrimination in the IFM process. In order to find the minima of the P_{loss} and P_{error} and the corresponding initial photon input states to reach them, we simplify the iteration of the quantum channels to transforming matrices operating on the pure state. With this compact simplification, the minimum properties of P_{loss} and P_{error} can be systemically studied. In addition, we show that the entangled photon input state cannot enhance the performance of IFM, considering P_{loss} and P_{error}, respectively.

Furthermore, we should point out that $P_f = P_{\text{loss}} + P_{\text{error}}$ is a more significant criterion to evaluate the IFM process, because it describes all the possibilities where the IFM process is a failure. It includes both the photon loss (object damage) and the error making in the discrimination process. However, even for this criterion P_f, we can also come to the conclusion that the quantum correlation (i.e., entanglement here) cannot benefit the IFM process (see Appendix D). In addition, the asymptotic behaviors are also studied and we find that the state $|1\rangle$ can perfectly detect the generic semitransparent object without any object damage when $N \to \infty$.

Finally, our paper provides theoretical support for the experimental research and practical realization of IFM, like

electron microscopy of biological substances or detection of fragile nanomaterials. Moreover, our theoretic approaches, borrowing from quantum information theory, such as quantum channel theory, quantum state discrimination, etc., can be applied to other quantum facilitating scenarios and the analysis of whether quantum correlation can benefit these specific processes or not is intriguing.

ACKNOWLEDGMENTS

We acknowledge C. R. Yang and X. Yuan for the insightful discussions. This paper was supported by the National Natural Science Foundation of China (Grant No. 11405093), Guangdong Innovative and Entrepreneurial Research Team Program (Grant No. 2016ZT06D348), and the Science, Technology, and Innovation Commission of Shenzhen Municipality (Grants No. ZDSYS20170303165926217 and No. JCYJ20170412152620376).

APPENDIX A: DERIVATION OF THE QUANTUM CHANNEL $\mathcal{E}_I$ OF THE GENERIC SEMITRANSPARENT OBJECT

In the main text, the generic semitransparent object is composed of a beamsplitter and a photon detector. The quantum channel $\mathcal{E}_I$ will be built by combing the operation of the beamsplitter and the photon detector in the following.

Let us give the channel description of the photon detector first. The photon detector is modeled by a two-level atom with ground state $|g\rangle$ and exited state $|e\rangle$. At first, the atom stays at $|g\rangle$, and it can interact with the incident photon mode, denoted by $|p\rangle$. Specifically, the atom absorbs the photon, transforms it to the vacuum state $|v\rangle$, and becomes the exited state $|e\rangle$ under the unitary $U_{\rm det}$; the state $|v,g\rangle$ keeps unchanged under the operation of $U_{\rm det}$, since there is no photon to excite the atom:

$$\begin{aligned} U_{\rm det}|p,g\rangle &= |v,e\rangle, \\ U_{\rm det}|v,g\rangle &= |v,g\rangle. \end{aligned} \tag{A1}$$

Explicitly, we write

$$U_{\rm det} = |v,e\rangle\langle p,g| + |p,g\rangle\langle v,e| + |v,g\rangle v,g| + |p,e\rangle\langle p,e|. \tag{A2}$$

Then after the interaction, the atom is measured in the $|g\rangle,|e\rangle$ basis and reset to $|g\rangle$. In fact, we do not need to concern ourselves with the operation of $U_{\rm det}$ on the other two states, say, $|p,e\rangle$ and $|v,e\rangle$, since the atom always stays at the ground state $|g\rangle$ before the interaction.

Consequently, the overall operation on the photon state is

$$\begin{aligned} \rho_{\rm out} &= \sum_{i=g,e} \langle i|U_{\rm det}(\rho_{\rm in}\otimes|g\rangle\langle g|)U_{\rm det}^{\dagger}|i\rangle \\ &= \sum_{i=g,e} \langle i|U_{\rm det}|g\rangle\rho_{\rm in}\langle g|U_{\rm det}^{\dagger}|i\rangle, \end{aligned} \tag{A3}$$

where $\rho_{\rm in}$ and $\rho_{\rm out}$ are the input and output photon states.

The above quantum operations in the summation of Eq. (A3) can be written down with Kraus operators as

$$\begin{aligned} K_0 &= \langle g|U_{\rm det}|g\rangle = |v\rangle\langle v|, \\ K_1 &= \langle e|U_{\rm det}|g\rangle = |v\rangle\langle p|, \end{aligned} \tag{A4}$$

and the quantum channel shows

$$\rho_{\rm out} = \sum_{i=0,1} K_i\rho_{\rm in}K_i^{\dagger}. \tag{A5}$$

For the scenario in the main text, there are three photon modes, i.e., $|1\rangle,|2\rangle,|3\rangle$, in addition to the vacuum mode $|v\rangle$. And only $|3\rangle$ can interact with the detector. So the quantum channel should be slightly modified to

$$\begin{aligned} \mathcal{E}_{\rm det}(\cdot) &= \sum_{i=0,1} D_i(\cdot)D_i^{\dagger}, \\ D_0 &= |1\rangle\langle 1| + |2\rangle\langle 2| + |v\rangle\langle v|, \\ D_1 &= |v\rangle\langle 3| \end{aligned} \tag{A6}$$

where D_0 and D_1 are the corresponding Kraus operators.

On the other hand, the matrix representation of the unitary for the beamsplitter $U_{\rm b}$ in the $|1\rangle,|2\rangle,|3\rangle,|v\rangle$ basis shows

$$U_{\rm b} = \begin{pmatrix} 1 & 0 & 0 & 0 \\ 0 & a & -\sqrt{1-a^2} & 0 \\ 0 & \sqrt{1-a^2} & a & 0 \\ 0 & 0 & 0 & 1 \end{pmatrix}. \tag{A7}$$

Combing the two operations of the photon detector $\mathcal{E}_{\rm det}$ and the beamsplitter U_b, we have the combined channel:

$$\mathcal{E}_{\rm com}(\cdot) = \sum_{i=0,1} D_iU_b(\cdot)U_b^{\dagger}D_i^{\dagger}, \tag{A8}$$

and the corresponding Kraus operators $C_i = D_iU_b$ show

$$\begin{aligned} C_0 &= |1\rangle\langle 1| + a|2\rangle\langle 2| - \sqrt{1-a^2}|2\rangle\langle 3| + |v\rangle\langle v|, \\ C_1 &= \sqrt{1-a^2}|v\rangle\langle 2| + a|v\rangle\langle 3|. \end{aligned} \tag{A9}$$

In fact, the component $|3\rangle$ is redundant as it is introduced to illustrate the intermediate process between the beamsplitter and the photon detector. Recall that the beamsplitter and the photon detector as a whole represent the semitransparent object, thus we can treat them together as a black box and the photon state in IFM equivalently lives in the three-dimensional space $\mathcal{H}_{12v} = \text{spanned}\{|1\rangle,|2\rangle,|v\rangle\}$.

As a result, without altering the function of the channel representing the semitransparent object, we can eliminate the terms in the above Kraus operator [Eq. (A9)] that relate to the component $|3\rangle$ and get

$$\begin{aligned} A_0 &= |1\rangle\langle 1| + a|2\rangle\langle 2| + |v\rangle\langle v|, \\ A_1 &= \sqrt{1-a^2}|v\rangle\langle 2|, \end{aligned} \tag{A10}$$

where we use A_0 and A_1 to denote the new Kraus operators.

Since all choices of which label to use to count the photon loss probability are equivalent, actually we can substitute the loss state $|3\rangle$ for the vacuum state $|v\rangle$ in the above Kraus operators to obtain the effective channel in the main text [Eq. (17)]. The physical insight behind this substitution is that the component $|3\rangle$ of the photon state reflected by the beamsplitter should be absorbed totally by the photon detector.

APPENDIX B: NONINCREASE OF THE GENERALIZED TRACE DISTANCE UNDER QUANTUM OPERATION

Here, we first give the definition of the generalized trace distance as follows.

Definition 1. The generalized trace distance of the two quantum states ρ_1 and ρ_2 shows

$$D_q(\rho_1,\rho_2) = \|q\rho_1 - (1-q)\rho_2\|, \tag{B1}$$

where $\|\cdots\|$ is the trace norm and $0 \leqslant q \leqslant 1$ is the corresponding probability factor.

Note that $D_{1/2}(\rho_1,\rho_2)$ is the original trace distance [28]. Then we show the property of the generalized trace distance in the following theorem.

Theorem 5. Suppose that $\Lambda(\cdot)$ is a trace preserving quantum operation, then it is contradictive for the generalized trace distance, i.e.,

$$D_q(\rho_1,\rho_2) \geqslant D_q(\Lambda(\rho_1),\Lambda(\rho_2)). \tag{B2}$$

To prove Theorem 5 conveniently, we show the following lemma.

Lemma 2. The trace norm of any Hermitian operator M shows

$$\|M\| = \mathrm{Tr}_{\max}[(P_1 - P_0)M], \tag{B3}$$

where the maximization is over all projector pairs P_0, P_1 that satisfy $P_0 + P_1 = \mathbb{I}$.

Proof. Since M is a Hermitian operator, we can choose a unitary U to diagonalize it to $UMU^\dagger$. And by separating the eigenvalues to non-negative and negative parts, we have $UMU^\dagger = Q' - S'$. As a result, M can be written as the subtraction of the two non-negative matrices $M = U^\dagger(Q' - S')U = Q - S$ and $\|M\| = \|Q - S\| = \mathrm{Tr}(Q) + \mathrm{Tr}(S)$, since Q and S live on orthogonal subspaces. Then, for any projector pair P_0, P_1,

$$\begin{aligned}\mathrm{Tr}[(P_1 - P_0)M] &= \mathrm{Tr}[(P_1 - P_0)(Q - S)]\\ &\leqslant \mathrm{Tr}[P_1 Q + P_0 S]\\ &\leqslant \mathrm{Tr}(Q) + \mathrm{Tr}(S)\\ &\leqslant \|M\|.\end{aligned} \tag{B4}$$

We can choose P_0 and P_1 as the projectors on the two orthogonal subspaces where Q and S live, respectively. Then $\mathrm{Tr}[(\Pi_1 - \Pi_0)M]$ can reach $\|M\|$ in this way and we finish the proof. ■

Now we prove Theorem 5 with the help of Lemma 2.

Proof.

$$\begin{aligned}\|M\| &= \mathrm{Tr}(Q) + \mathrm{Tr}(S)\\ &= \mathrm{Tr}[\Lambda(Q) + \Lambda(S)]\\ &\geqslant \mathrm{Tr}\{(P_1' - P_0')[\Lambda(Q) - \Lambda(S)]\}\\ &= \mathrm{Tr}[(P_1' - P_0')\Lambda(M)]\\ &= \|\Lambda(M)\|,\end{aligned} \tag{B5}$$

where P_0' and P_1' form the projector pair used to reach the maximal value $\|\Lambda(M)\|$ for the Hermitian operator $\Lambda(M)$, referring to Lemma 2. Then, by substituting $M = q\rho_1 - (1-q)\rho_2$, we finish the proof. ■

APPENDIX C: PROOF OF LEMMA 1

Here, we give the proof of Lemma 1 in the main text:

$$\|p|\psi_1\rangle\langle\psi_1| - |\psi_2\rangle\langle\psi_2|\| = \sqrt{(p+1)^2 - 4p|\langle\psi_1|\psi_2\rangle|^2}.$$

Proof. In general $|\psi_1\rangle$ and $|\psi_2\rangle$ span a two-dimensional Hilbert space. Since $|\psi_2\rangle\langle\psi_2|$ stays invariant if we change the global phase of it, without loss of generality,

$$|\psi_2\rangle = \cos\frac{\gamma}{2}|\psi_1\rangle + \sin\frac{\gamma}{2}|\psi_3\rangle \ (0 \leqslant \gamma \leqslant \pi/2). \tag{C1}$$

Here $|\psi_3\rangle$ is orthogonal to $|\psi_1\rangle$, and they constitute the basis of the space.

Then, we have the Bloch sphere representation of $|\psi_1\rangle$ and $|\psi_2\rangle$ in the basis $\{|\psi_1\rangle,|\psi_3\rangle\}$:

$$\begin{aligned}|\psi_1\rangle\langle\psi_1| &= \tfrac{1}{2}(\mathbb{I} + \sigma_z),\\ |\psi_2\rangle\langle\psi_2| &= \tfrac{1}{2}(\mathbb{I} + \cos\gamma\sigma_z + \sin\gamma\sigma_x).\end{aligned} \tag{C2}$$

Thus the trace norm shows

$$\begin{aligned}&\|p|\psi_1\rangle\langle\psi_1| - |\psi_2\rangle\langle\psi_2|\|\\ &\quad= \tfrac{1}{2}\|(p-1)\mathbb{I} + (p - \cos\gamma)\sigma_z - \sin\gamma\sigma_x\|.\end{aligned} \tag{C3}$$

The two eigenvalues of $(p-1)\mathbb{I} + (p-\cos\gamma)\sigma_z - \sin\gamma\sigma_x$ are $(p-1) \pm \sqrt{(p-\cos\gamma)^2 + \sin^2\gamma}$. Hence,

$$\begin{aligned}\|p|\psi_1\rangle\langle\psi_1| - |\psi_2\rangle\langle\psi_2|\| &= \sqrt{(p-\cos\gamma)^2 + \sin^2\gamma}\\ &= \sqrt{(p+1)^2 - 4p\cos^2\frac{\gamma}{2}}\\ &= \sqrt{(p+1)^2 - 4p|\langle\psi_1|\psi_2\rangle|^2}.\end{aligned} \tag{C4}$$

■

APPENDIX D: EFFECT OF QUANTUM CORRELATION FOR THE IFM PROCESS CONSIDERING P_{error} and P_f

In this appendix, we give the detailed illustration of the argument in the main text that quantum correlation cannot benefit the IFM process considering P_{error} and P_f, respectively.

For simplicity, we substitute for the terms in Eq. (78)

$$\begin{aligned}\lambda_1 &= q\mathrm{Tr}[C^\dagger C\rho_A] + (1-q),\\ \lambda_2 &= 2\sqrt{q(1-q)}|\mathrm{Tr}[D^\dagger C\rho_A]|\end{aligned} \tag{D1}$$

As a result, Eq. (78) becomes to a more concise form

$$P_{\mathrm{error}} = \frac{1}{2}\left(\lambda_1 - \sqrt{\lambda_1^2 - \lambda_2^2}\right). \tag{D2}$$

Due to the first-order partial derivative on λ_1 of P_{error} being

$$\frac{\partial P_{\mathrm{error}}}{\partial\lambda_1} = \frac{1}{2}\left(1 - \frac{\lambda_1}{\sqrt{\lambda_1^2 - \lambda_2^2}}\right) \leqslant 0, \tag{D3}$$

P_{error} monotonically decreases with the increasing of λ_1. In the meantime, it is obvious that P_{error} decreases with the decreasing of λ_2. Consequently, increasing λ_1 and decreasing λ_2 at the same time can minimize P_{error}.

Here, with the help of Eqs. (70), (75), and (76), we present the expressions for $\mathrm{Tr}[C^\dagger C\rho_A]$ and $\mathrm{Tr}[D^\dagger C\rho_A]$ in the definitions of λ_1 and λ_2 explicitly as

$$\begin{aligned}\mathrm{Tr}[C^\dagger C\rho_A] &= \left(\frac{1-a}{2}\right)^{2N}\left[f_1^2\left(1+k_1^2\right)+f_2^2\right.\\ &\quad\left.+2f_1(f_2r_z-f_1k_1r_x)\right],\\ \mathrm{Tr}[D^\dagger C\rho_A] &= \left(\frac{1-a}{2}\right)^{N}[f_1k_1-f_1r_x+if_2r_y]. \end{aligned}\tag{D4}$$

The above equations show that for a fixed r_x we can always increase λ_1 and decrease λ_2 (i.e., decrease P_{error}) by changing $r_y=0$ and $r_z=\sqrt{1-r_x^2}$. In other words, the minimum of P_{error} should be reached by pure state $\rho_A=|\varphi_A\rangle\langle\varphi_A|$ of the photon A part. Thus, the entangled photon input state cannot enhance the performance for P_{error} in all k_1 regimes, compared with the single-photon input state.

Moreover, we consider the effect of quantum correlation to the IFM process, with a more effective criterion $P_f=P_{\mathrm{loss}}+P_{\mathrm{error}}$. This describes all the failure probability in the IFM process. Owing to Theorem 1, P_f also shows the following concave property like P_{error}:

$$P_f\geqslant\sum_i p_iP_f^i.\tag{D5}$$

That is to say, the minimum of P_f should also be reached by the pure state and the quantum correlation here means entanglement. With the help of Eqs. (69), (78), and (D1), we have P_f:

$$P_f=1-\frac{1}{2}\left(\lambda_1+\sqrt{\lambda_1^2-\lambda_2^2}\right).\tag{D6}$$

P_f also decreases with the increasing of λ_1 and decreasing of λ_2. Consequently, just like the aforementioned reason for P_{error}, we can also argue that entanglement cannot enhance the performance of IFM considering P_f.

APPENDIX E: DERIVATION OF EQ. (81)

Here, we give the derivation of $(P_{\mathrm{loss}})_{\mathrm{min}}^{N\to\infty}$ in Eq. (81), which is the asymptotic behavior of Eq. (71) as $N\to 0$.

First, utilizing the same approximation technique used in Eq. (79) in the main text, we get

$$\begin{aligned}&\left(\frac{1-a}{2}\right)^N(\Sigma_2-\Sigma_1)=O(a^N)\to 0,\\ &\left(\frac{1-a}{2}\right)^N\Sigma_1\simeq\left(\frac{1-a}{2}\right)^N\Sigma_2\\ &\qquad=\frac{1}{2}-\frac{1+a}{1-a}\frac{\pi^2}{16N}+O\left(\frac{1}{N^3}\right).\end{aligned}\tag{E1}$$

Then, let us consider the asymptotic behavior of the minimum of P_{loss} in Eq. (71). By applying Eq. (65) and (67) and the definitions of k_1 and k_2 [Eq. (61)], we have

$$\begin{aligned}&\left(\frac{1-a}{2}\right)^{2N}\left(f_1+\sqrt{f_2^2+f_1^2k_1^2}\right)^2\\ &\simeq\left(\frac{1-a}{2}\right)^{2N}\left(f_1+f_2+\frac{f_1^2}{2f_2}k_1^2\right)^2\\ &=\left(\frac{1-a}{2}\right)^{2N}\left(\frac{\Sigma_1}{\sqrt{1-k_1^2}}+\Sigma_2+\frac{\Sigma_1^2}{2\Sigma_2}\frac{k_1^2}{1-k_1^2}\right)^2\\ &\simeq\left(\frac{1-a}{2}\right)^{2N}\left[\Sigma_1\left(1+\frac{k_1^2}{2}\right)+\Sigma_2+\frac{\Sigma_1^2}{2\Sigma_2}k_1^2\left(1+k_1^2\right)\right]^2\\ &\simeq\left(\frac{1-a}{2}\right)^{2N}\left[(\Sigma_1+\Sigma_2)+\frac{k_1^2}{2}\Sigma_1\left(1+\frac{\Sigma_1}{\Sigma_2}\right)\right]^2\\ &\simeq\left[1-\frac{1+a}{1-a}\frac{\pi^2}{8N}+\left(\frac{1+a}{1-a}\right)^2\frac{\pi^2}{8N^2}+O\left(\frac{1}{N^3}\right)\right]^2\\ &\simeq 1-\frac{1+a}{1-a}\frac{\pi^2}{4N}+O\left(\frac{1}{N^2}\right),\end{aligned}\tag{E2}$$

where in the next-to-last row we employ the equalities in Eq. (E1). So the asymptotic expression of Eq. (71) is

$$(P_{\mathrm{loss}})_{\mathrm{min}}^{N\to\infty}\simeq q\left[\frac{1+a}{1-a}\frac{\pi^2}{4N}-O\left(\frac{1}{N^2}\right)\right].$$

[1] M. Renninger, Z. Phys. **158**, 417 (1960).
[2] R. H. Dicke, Am. J. Phys **49**, 925 (1981).
[3] A. C. Elitzur and L. Vaidman, Found. Phys. **23**, 987 (1993).
[4] P. Kwiat, H. Weinfurter, T. Herzog, A. Zeilinger, and M. A. Kasevich, Phys. Rev. Lett. **74**, 4763 (1995).
[5] B. Misra and E. C. G. Sudarshan, J. Math. Phys. **18**, 756 (1977).
[6] P. G. Kwiat, A. G. White, J. R. Mitchell, O. Nairz, G. Weihs, H. Weinfurter, and A. Zeilinger, Phys. Rev. Lett. **83**, 4725 (1999).
[7] A. Karlsson, G. Björk, and E. Forsberg, Phys. Rev. Lett. **80**, 1198 (1998).
[8] J. Volz, R. Gehr, G. Dubois, J. Estève, and J. Reichel, Nature (London) **475**, 210 (2011).
[9] S. Inoue and G. Björk, J. Opt. B **2**, 338 (2000).
[10] W. P. Putnam and M. F. Yanik, Phys. Rev. A **80**, 040902 (2009).
[11] S. Thomas, C. Kohstall, P. Kruit, and P. Hommelhoff, Phys. Rev. A **90**, 053840 (2014).
[12] P. Kruit, R. Hobbs, C.-S. Kim, Y. Yang, V. Manfrinato, J. Hammer, S. Thomas, P. Weber, B. Klopfer, C. Kohstall, T. Juffmann, M. Kasevich, P. Hommelhoff, and K. Berggren, Ultramicroscopy **164**, 31 (2016).
[13] G. S. Paraoanu, Phys. Rev. Lett. **97**, 180406 (2006).
[14] L. Chirolli, E. Strambini, V. Giovannetti, F. Taddei, V. Piazza, R. Fazio, F. Beltram, and G. Burkard, Phys. Rev. B **82**, 045403 (2010).
[15] O. Zilberberg, A. Romito, and Y. Gefen, Phys. Rev. B **93**, 115411 (2016).
[16] M. Hafner and J. Summhammer, Phys. Lett. A **235**, 563 (1997).

[17] T. Tsegaye, E. Goobar, A. Karlsson, G. Björk, M. Y. Loh, and K. H. Lim, Phys. Rev. A **57**, 3987 (1998).
[18] X.-s. Ma, X. Guo, C. Schuck, K. Y. Fong, L. Jiang, and H. X. Tang, Phys. Rev. A **90**, 042109 (2014).
[19] J. C. García-Escartín and P. Chamorro-Posada, arXiv:quant-ph/0512019.
[20] G. Mitchison and S. Massar, Phys. Rev. A **63**, 032105 (2001).
[21] J.-S. Jang, Phys. Rev. A **59**, 2322 (1999).
[22] L. Vaidman, Found. Phys. **33**, 491 (2003).
[23] P. G. Kwiat, Phys. Scr. **T76**, 115 (1998).
[24] H. Azuma, Phys. Rev. A **74**, 054301 (2006).
[25] S. Lloyd, Science **321**, 1463 (2008).
[26] C. W. Helstrom, *Quantum Detection and Estimation Theory* (Academic, New York, 1976), Vol. 123.
[27] U. Herzog, J. Opt. B **6**, S24 (2004).
[28] M. A. Nielsen and I. L. Chuang, *Quantum Computation and Quantum Information* (Cambridge University, Cambridge, England, 2010).
[29] S. L. Braunstein, C. M. Caves, and G. Milburn, Ann. Phys. **247**, 135 (1996).
[30] V. Giovannetti, S. Lloyd, and L. Maccone, Phys. Rev. Lett. **96**, 010401 (2006).